Notch1 counteracts WNT/β-catenin signaling through chromatin modification in colorectal cancer

Hyun-A Kim, … , Daehee Hwang, Young-Yun Kong

Research Article   **Oncology**

Crosstalk between the Notch and wingless-type MMTV integration site (WNT) signaling pathways has been investigated for many developmental processes. However, this negative correlation between Notch and WNT/β-catenin signaling activity has been studied primarily in normal developmental and physiological processes in which negative feedback loops for both signaling pathways are intact. We found that Notch1 signaling retained the capability of suppressing the expression of WNT target genes in colorectal cancers even when β-catenin destruction by the adenomatous polyposis coli (APC) complex was disabled. Activation of Notch1 converted high-grade adenoma into low-grade adenoma in an *Apc^{min}* mouse colon cancer model and suppressed the expression of WNT target genes in human colorectal cancer cells through epigenetic modification recruiting histone methyltransferase SET domain bifurcated 1 (SETDB1). Extensive microarray analysis of human colorectal cancers also showed a negative correlation between the Notch1 target gene, Notch-regulated ankyrin repeat protein 1 (NRARP), and WNT target genes. Notch is known to be a strong promoter of tumor initiation, but here we uncovered an unexpected suppressive role of Notch1 on WNT/β-catenin target genes involved in colorectal cancer.

Find the latest version:

https://jci.me/61216/pdf

Notch1 counteracts WNT/β-catenin signaling through chromatin modification in colorectal cancer

Hyun-A Kim,[1] Bon-Kyoung Koo,[1] Ji-Hoon Cho,[2] Yoon-Young Kim,[1,3] Jinwoo Seong,[1] Hee Jin Chang,[4] Young Min Oh,[3] Daniel E. Stange,[5] Jae-Gahb Park,[4] Daehee Hwang,[2] and Young-Yun Kong[1]

[1]Department of Biological Sciences, College of Natural Sciences, Seoul National University, Seoul, Republic of Korea.
[2]School of Interdisciplinary Bioscience and Bioengineering, and [3]Division of Molecular and Life Sciences, Pohang University of Science and Technology, Pohang, Republic of Korea. [4]Research Institute and Hospital, National Cancer Center, Goyang, Gyeonggi, Republic of Korea. [5]Hubrecht Institute-KNAW (Royal Netherlands Academy of Arts and Sciences) and University Medical Center Utrecht, Utrecht, The Netherlands.

Crosstalk between the Notch and wingless-type MMTV integration site (WNT) signaling pathways has been investigated for many developmental processes. However, this negative correlation between Notch and WNT/β-catenin signaling activity has been studied primarily in normal developmental and physiological processes in which negative feedback loops for both signaling pathways are intact. We found that Notch1 signaling retained the capability of suppressing the expression of WNT target genes in colorectal cancers even when β-catenin destruction by the adenomatous polyposis coli (APC) complex was disabled. Activation of Notch1 converted high-grade adenoma into low-grade adenoma in an *Apc^min* mouse colon cancer model and suppressed the expression of WNT target genes in human colorectal cancer cells through epigenetic modification recruiting histone methyltransferase SET domain bifurcated 1 (SETDB1). Extensive microarray analysis of human colorectal cancers also showed a negative correlation between the Notch1 target gene, Notch-regulated ankyrin repeat protein 1 (NRARP), and WNT target genes. Notch is known to be a strong promoter of tumor initiation, but here we uncovered an unexpected suppressive role of Notch1 on WNT/β-catenin target genes involved in colorectal cancer.

Introduction

Activation of the adenomatous polyposis coli/β-catenin (APC/β-catenin) pathway is a crucial initiating event in human colorectal cancer (CRC) (1, 2). The multistage progression of CRC is then followed by sequential activation of oncogenes and inactivation of tumor-suppressor genes, including *K-RAS*, *TGFβ*/*SMAD4*, and *TP53* (2, 3). Although the implications of these genetic alterations are well characterized in the adenoma-carcinoma sequence, limited studies have been conducted to examine the influence of other molecular signaling pathways on these tumors.

Signaling pathways, such as wingless-type MMTV integration site (WNT), BMP, Hedgehog, and Notch, are important not only in embryonic development, but also in adult intestinal homeostasis (4, 5). In the intestine, WNT signaling is crucial for the proliferation and maintenance of intestinal stem cells and progenitor cells (6). Notch signaling regulates cell fate decisions between secretory and absorptive cell lineages (7, 8). The Notch signaling pathway also plays a role in the maintenance of proliferating progenitors (9, 10). Under normal conditions, these 2 pathways are exclusively required for maintaining intestinal stem cells (7). Activation of the WNT/β-catenin signaling pathway is the main rate-limiting step of CRC initiation (1), and Notch signaling has been shown to promote CRC initiation in a mouse *Apc^min* tumor model (11, 12). Therefore, the Notch and WNT pathways may function cooperatively in intestinal epithelium and tumors.

γ-Secretase inhibitor has been utilized to prevent intestinal tumor growth in *Apc^min* mice (10), which showed reduced proliferation of tumor cells and increased goblet cell conversion following γ-secretase inhibitor treatment. In contrast, overexpression of the Notch intracellular domain facilitates tumor formation in *Apc^min* mice (11), suggesting an oncogenic role of Notch in intestinal tumor formation. However, other reports have examined the efficacy of γ-secretase inhibitors in blocking the growth of CRCLs and have obtained disappointing results (13). A genetic analysis involving *Apc* and *Rbpjκ* floxed mice also failed to demonstrate that Notch signaling is essential for tumorigenic transformation (14), and the *Apc;Rbpjκ* compound mice did not show a survival advantage. Thus, the precise role of Notch signaling in CRCs is controversial.

We investigated the role of Notch signaling in established CRC tumors. We did not examine this signaling during the initial phase of transformation because it has been clearly shown in many studies that Notch signaling promotes the onset of intestinal tumors (11). Thus, after tumor onset, we reexamined the characteristics of Notch-activated tumors in *RosaN1^{+/RN1};Apc^min* mice in which tumor initiation had progressed compared with *Apc^min* mice (11). Unexpectedly, these tumors showed low-grade adenoma features, including columnar epithelial morphology and a restoration of the adherens junction. Concomitant microarray analysis demonstrated Notch-mediated downregulation of Tcf4/β-catenin target genes, even in the absence of functional Apc. Microarray analysis of human CRC patient data further reinforced the negative correlation between Notch and WNT signaling activity in CRC. Our study examining the effect of Notch signaling in CRC cell lines (CRCLs) revealed that Notch signaling leads to a repressive
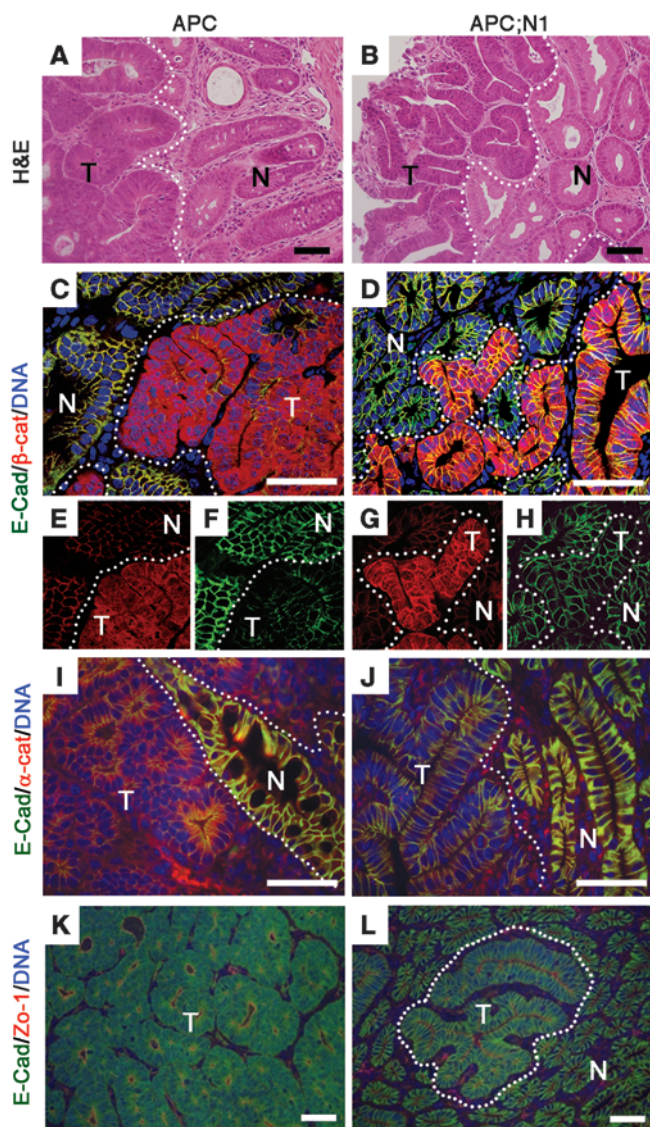
Figure 1
Notch-activated *Apc^min* tumors show low-grade adenoma features. Colons from 10- to 15-week-old *Apc^min* (APC: **A**, **C**, **E**, **F**, **I**, and **K**) and 7-week-old *Vil-Cre;RosaN1^+/RN1;Apc^min* (APC;N1: **B**, **D**, **G**, **H**, **J**, and **L**) mice were used for histological analysis. Note that APC;N1 tumors have well-branched tubular structures (**B**), and more membranous β-catenin (**G**) and E-cadherin (**H**) staining with extended apical membranes (**L**) compared with APC tumors. Staining: H&E (**A** and **B**); E-cadherin (E-cad) (green), and β-catenin (β-cat) (red) (**C**, **D**, **E**, **F**, **G**, and **H**); E-cadherin (green) and α-catenin (red) (**I** and **J**); and E-cadherin (green) and ZO-1 (red) (**K** and **L**). N, normal tissue; T, tumor. Dotted lines indicate tumor regions. Scale bars: 50 μm.

available online with this article; doi:10.1172/JCI61216DS1). Consistent with the results of a previous study (11), 7-week-old *Vil-Cre;RosaN1^+/RN1;Apc^min* mice developed several tumors in their small and large intestines, while tumors were not or were rarely detected in control *Apc^min* mice. Since the onset of tumor formation was clearly accelerated in *Vil-Cre;RosaN1^+/RN1;Apc^min* mice compared with control *Apc^min* mice in our study as well as in a previous study (11), we collected tumor tissues from 7-week-old *Vil-Cre;RosaN1^+/RN1;Apc^min* mice and 10- to 15-week-old *Apc^min* mice. For histological analysis, we used tumors of similar size from each genotype for comparison.

Interestingly, a detailed histological analysis of tumors in *Vil-Cre;RosaN1^+/RN1;Apc^min* mice, particularly those in the colon, showed low-grade adenoma characteristics with enhanced epithelial cell morphology, while control tumors from *Apc^min* mice showed high-grade adenoma characteristics (Figure 1, A and B). Tumors from *Vil-Cre;RosaN1^+/RN1;Apc^min* mice did not form tightly packed cell agglomerations as observed in *Apc^min* tumors. Instead, they formed an extended single layer of epithelial cells. Low-grade adenoma characteristics were also observed in older (10- to 15-week-old) moribund *Vil-Cre;RosaN1^+/RN1;Apc^min* mice (not shown), suggesting that mortality of *Vil-Cre;RosaN1^+/RN1;Apc^min* mice was not due to further progression of tumor severity.

Next, we investigated the localization of β-catenin. Control *Apc^min* tumors showed prominent nuclear and cytoplasmic staining of β-catenin, a hallmark of active WNT signaling (Figure 1, C and D). Although nuclear β-catenin was still detectable in Notch-activated *Apc^min* tumors, most of the β-catenin was present in the plasma membrane (Figure 1, F and G). Importantly, the expression level of E-cadherin was restored in the plasma membrane of Notch-activated *Apc^min* tumors (Figure 1, E and H). Coimmunostaining with E-cadherin and α-catenin showed that, while adherens junctions were disrupted in *Apc^min* tumors (Figure 1I), E-cadherin and α-catenin were colocalized in the plasma membrane of Notch-activated *Apc^min* tumors (Figure 1J). Moreover, double staining of E-cadherin and ZO-1, a marker for tight junctions, clearly showed that lateral and apical membranes were well established in Notch-activated *Apc^min* tumors (Figure 1, K and L). These results show that Notch-activated *Apc^min* tumors display low-grade adenoma with restored epithelial characteristics.

Downregulated WNT target genes in Notch-activated Apc^min tumors. Milder histological characteristics of Notch-activated *Apc^min* tumors compared with those of normal *Apc^min* tumors prompted us to further analyze molecular changes in these tumor models. Because tumor onset was accelerated in the *Vil-Cre;RosaN1^+/RN1; Apc^min* mice as described above, we collected tumors of similar

histone status of WNT target gene promoters through the activities of Nemo-like kinase (NLK) and SET domain bifurcated 1 (SETDB1). While Notch signaling is a strong promoter in intestinal tumor initiation, it also has an unexpected suppressive role in the expression of WNT/β-catenin target genes in established tumors, even in the absence of functional Apc.

Results

Histological characterization of Notch-activated Apc^min tumor after its onset. To examine how Notch activation affects intestinal tumors, we generated an intestinal gain-of-Notch model by crossing *Apc^min* background mice with *Rosa-N1icd* (*RN1*) mice, which have a transgene composed of a floxed Neo/STOP cassette followed by N1ICD without the PEST domain in the *Rosa26* locus (15) and the *Villin-Cre* (*Vil-Cre*) transgene (16). These mice contain Notch-activated intestinal epithelium in which intestinal tumors occur upon the loss of heterogeneity of the *Apc^min* locus. A detailed description of these mice is provided in Supplemental Information and in Supplemental Figure 1 (supplemental material
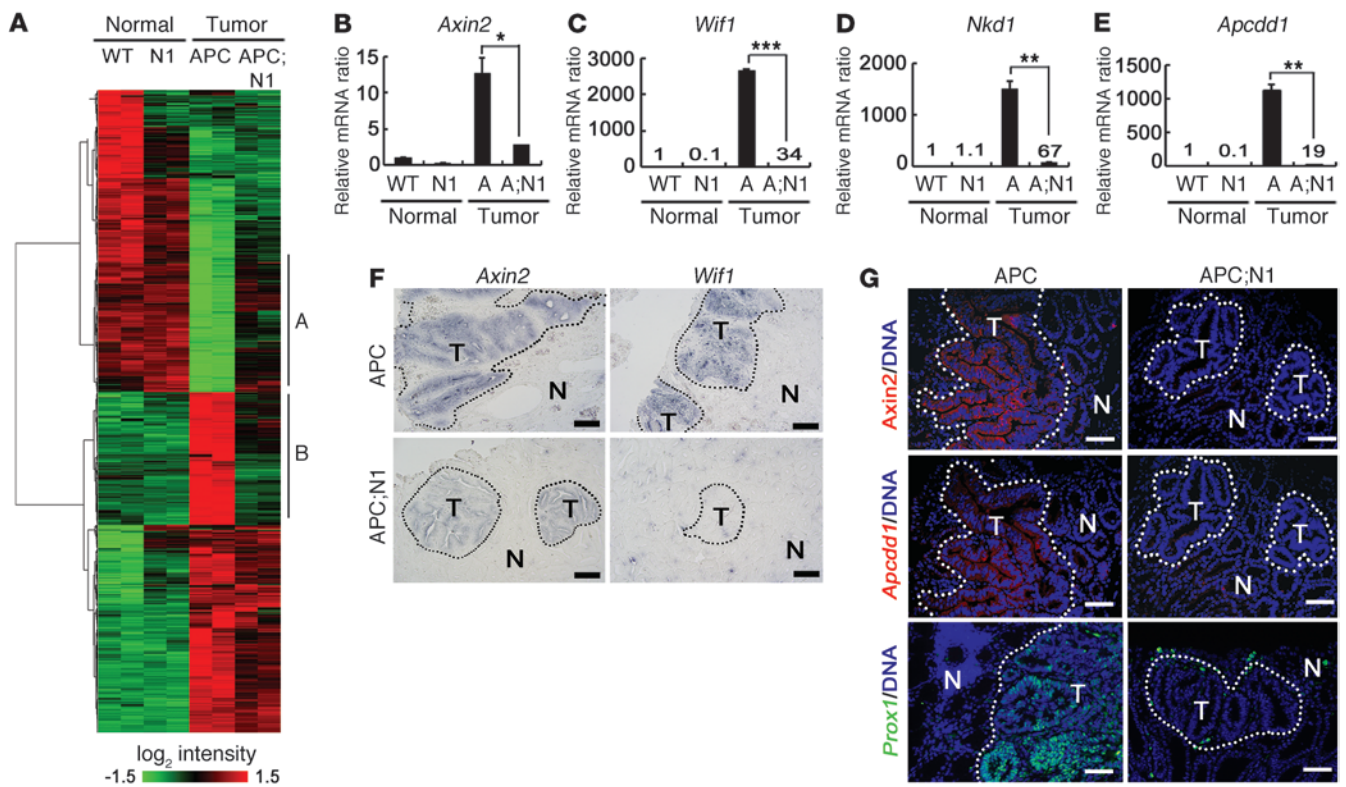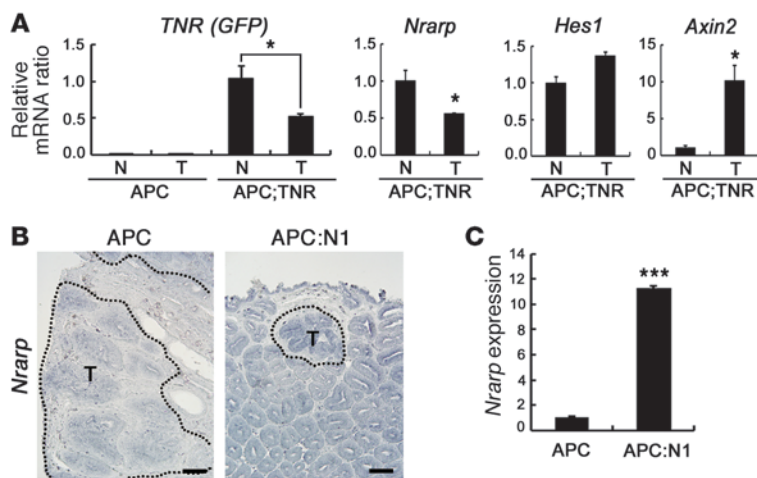
Figure 2
Decreased levels of WNT target genes in Notch-activated *Apc^min* tumors. Colons (normal) from 10-week-old WT and 7-week-old *Vil-Cre;RosaN1^{+/RN1}* (N1) mice and colonic tumor tissues (tumor) from 10-week-old *Apc^min* (APC) and 7-week-old *Vil-Cre;RosaN1^{+/RN1};Apc^min* mice were used for gene expression and histological analysis. (**A**) Heat map of gene expression levels. Clusters A and B indicate genes that reverted to levels in normal tissues upon Notch activation in the tumors. (**B–E**) Real-time qRT-PCR analysis (**B–E**). Note the reduced expression levels of WNT target genes (*Axin2*, *Wif1*, *Nkd1*, and *Apcdd1*) in APC;N1 tumors compared with those of APC tumors. Bars indicate mean + SD. *$P < 0.05$; **$P < 0.01$; ***$P < 0.001$. (**F** and **G**) In situ hybridization (**F**) and fluorescent immunostaining (**G**) of *Apc^min* (upper panels) and *Vil-Cre;RosaN1^{+/RN1};Apc^min* (lower panels) tumors. Note that the expression levels of *Axin2*, *Wif1*, *Apcdd1*, and *PROX1* were reduced or absent in *Vil-Cre;RosaN1^{+/RN1};Apc^min* tumors. Dotted lines indicate tumor regions. Scale bars: 100 μm (**F**); 50 μm (**G**).

size from 7-week-old *Vil-Cre;RosaN1^{+/RN1};Apc^min* mice and 10-week-old *Apc^min* mice. First, we determined the changes in expression between tumors from these 2 genotypes and then compared the entire signature to changes between normal intestinal epithelium and *Apc^min* tumors (Figure 2A and Supplemental Table 1). Among 2,750 genes significantly altered during *Apc^min* tumorigenesis (normal tissue vs. tumor), activation of Notch signaling suppressed approximately 40% of tumor-associated genes toward normal levels (Figure 2A). In cluster A, depicted in the figure, we identified genes related to cell metabolism and differentiation using Kyoto Encyclopedia of Genes and Genomes (KEGG) pathway analysis, confirming the histological observation that Notch signaling promotes epithelial differentiation of intestinal tumor cells (Supplemental Table 2).

Strikingly, the KEGG pathway analysis of cluster B showed that WNT signaling pathway genes were downregulated in Notch-activated tumors (Supplemental Table 3; $P = 1.3 \times 10^{-4}$). Quantitative RT-PCR (qRT-PCR) analysis confirmed that the WNT target genes *Axin2*, *Wif1*, *Nkd1*, and *Apcdd1* (17–20) were downregulated in Notch-activated *Apc^min* tumors compared with normal *Apc^min* tumors (Figure 2, B–E). Consistent with these results, in situ hybridization and immunohistological analysis clearly showed that expression

levels of *Axin2*, *Wif1*, and *Apcdd1* were reduced in Notch-activated *Apc^min* tumors (Figure 2, F and G). Importantly, we also observed that *PROX1*, a β-catenin target gene known to promote intestinal tumor progression (21), was nearly absent in Notch-activated *Apc^min* tumors (Figure 2G). These data show that Notch signaling specifically counteracts deregulation of approximately 40% of *Apc^min* tumor-associated genes by modulating factors downstream of the WNT signaling pathway.

Negative correlation between Notch and WNT target genes in colonic tumors in mice and humans. Based on our observations using mouse tumor models, we explored gene expression profiles of human CRC patients to determine whether similar features, such as the negative correlation between Notch and WNT target genes, could also be observed in human CRC. To address this issue, we first sought to identify a reliable marker gene for Notch signaling activity. Although *Hes1* is a well-known Notch target gene, a recent study reported that *Hes1* is also directly transcribed by β-catenin signaling through conserved Tcf motifs as well as Notch (14). We also did not observe a clear correlation in *Hes1* expression between control and Notch-activated *Apc^min* tumors (Figure 3A). Therefore, we sought to identify another known Notch target gene and identified Notch-regulated ankyrin repeat protein 1 (*Nrarp*) from

Figure 3
Nrarp represents Notch signaling activity in intestinal tumors. (**A**) Real-time qRT-PCR analysis of Notch target genes (GFP of TNR, *Nrarp*, and *Hes1*) and WNT target gene (*Axin2*) in normal and tumor tissues from 15-week-old *Apc* and *Apc^min;TNR* (*Apc;TNR*) mice. Note that Notch activity (TNR) was well correlated with the expression level of *Nrarp*, but not *Hes1*. Bars indicate mean + SD. *P < 0.05. (**B** and **C**) In situ hybridization (**B**) and real-time qRT-PCR (**C**) analysis of *Nrarp* in the colonic tumor tissues from *Apc* and *Vil-Cre;RosaN1^+/RN1;Apc^min* mice. Dotted lines indicate tumor regions (**B**). Scale bars: 100 μm. Bars indicate mean + SD. ***P < 0.001.

our mouse models as reported (22–24). To confirm the correlation between *Nrarp* expression and Notch signaling activity, we used transgenic Notch reporter (*TNR*) mice, which have a Notch-responsive GFP reporter that faithfully recapitulates endogenous Notch activity (25). In *Apc^min;TNR* mice, expression levels of *GFP* and *Nrarp* were reduced to approximately half in the tumor compared with nontumor intestinal epithelial tissues, while the expression level of *Hes1* slightly increased (Figure 3A). Consistently, in situ hybridization and real-time qRT-PCR analysis showed that the *Nrarp* expression level was increased in Notch-activated *Apc^min* tumors compared with normal *Apc^min* tumors (Figure 3, B and C). These data show that *Nrarp* reports Notch signaling activity more accurately than *Hes1* in intestinal tumors.

Using *Nrarp* as an indicator of Notch signaling activity in CRC, we used both Pearson's and Spearman's correlation analysis (P ≤ 0.05; see Methods) to identify genes correlated with *Nrarp* in 2 independent human microarray data sets (GEO GSE5206 and GSE2109). These data sets contained a sufficient amount of human patient data to perform our statistical analysis. Coexpression analysis provided a set of genes whose expression was positively or negatively correlated with *Nrarp* (human *Nrarp* CO-DEG, where DEG indicates differentially expressed gene) expression. If the *Nrarp* expression level accurately predicts Notch activity in human CRC, genes that are filtered using this coexpression analysis would be similar to genes identified by comparing control and Notch-activated *Apc^min* tumors. We analyzed genes that commonly occur in mouse Notch DEG sets between control and Notch-activated *Apc^min* tumors (Supplemental Table 1; P < 0.05, 2-fold) and human *Nrarp* CO-DEG (genes that correlate with *Nrarp*; P ≤ 0.05) (Supplemental Table 4; 239 genes coregulated in mouse Notch-DEG and human *Nrarp* CO-DEG). The heat map of these genes, sorted based on the expression level of *Nrarp*, showed an 85.8% identical expression change between mouse and human (Figure 4A), suggesting that *Nrarp* is a reliable marker for Notch signaling activity in human CRC. Genes associated with the differentiation of intestinal epithelium, *CDX1* and *CDX2*, showed higher expression levels in *Nrarp^hi* human colonic tumors (Figure 4B and ref. 26). *VIMENTIN* (27) and *PROX1*, which are associated with tumorigenic activities such as EMT and tumor progression, exhibited lower levels of expression in *Nrarp^hi* human colonic tumors (Figure 4B). In particular, a negative correlation between *Nrarp* and *PROX1*, a known WNT target gene important in CRC progression,

further supports our previous observation that Notch signaling can attenuate WNT/β-catenin activity under destruction complex–deregulated conditions.

Next, to investigate Notch signaling activity during CRC development in humans, we compared *Nrarp* expression levels among 3 human microarray data sets. *Nrarp* expression was significantly decreased along with human CRC progression (Figure 4C; GEO GSE5206, normal to adenoma, adenocarcinoma). Although the stepwise differences were minor, the overall pattern showed a significant decrease in expression (Figure 4C; P = 0.0002 using 1-way ANOVA). Data sets (GEO GSE4107 and GSE8671) were used to confirm the reduction of *Nrarp* expression in carcinomas compared with that of normal intestinal epithelium (Figure 4C; P = 0.0012 and P < 0.0001, respectively). Recently, Smith et al. reported microarray data coupled with patient survival information (GEO GSE17538) (28). We divided this patient data into 2 groups, *Nrarp^hi* (upper 25%) and *Nrarp^mid/lo*, and constructed a Kaplan–Meier plot (Figure 4D). Interestingly, significantly longer and higher survival was observed for patients with high *Nrarp* expression, suggesting that *Nrarp* expression is a strong predictor of patient survival (P = 0.022). Based on *Nrarp* expression as a surrogate marker, we show that Notch activity in CRCs decreases during CRC progression.

Notch signaling suppresses the expression of WNT target genes in human CRC cells. To further investigate the crosstalk between Notch and WNT signaling, we sorted *Nrarp* in human CRCLs based on *Nrarp* expression levels. Interestingly, *Nrarp^hi* CRCLs highly expressed *CDX1* and *CDX2*, but did not express or only minimally expressed *VIMENTIN* and *PROX1* (Figure 5A). In contrast, *Nrarp^lo/–* CRCLs highly expressed *VIMENTIN* and *PROX1*, but did not express or only minimally expressed *CDX1* and *CDX2* (Figure 5A). In order to determine whether Notch signaling is really active in the *Nrarp^hi* CRCLs, but not in *Nrarp^lo/–* CRCLs, we examined the expression of cleaved Notch1. As expected, cleaved Notch1 was readily detected in the *Nrarp^hi* CRCLs, such as SNU61 and LOVO, but not in *Nrarp^lo/–* CRCLs, such as SW620 and COLO205 (Figure 5B). In order to investigate whether the *NRARP* expression is directly induced by Notch signaling, we tested the effect of cycloheximide, a new protein synthesis inhibitor, on Notch signaling-induced *NRARP* expression in SNU61 and LOVO cells. The decrease of NRARP expression by γ-secretase inhibitor (DAPT) treatment in SNU61 and LOVO cells was reverted by washout of DAPT in the absence
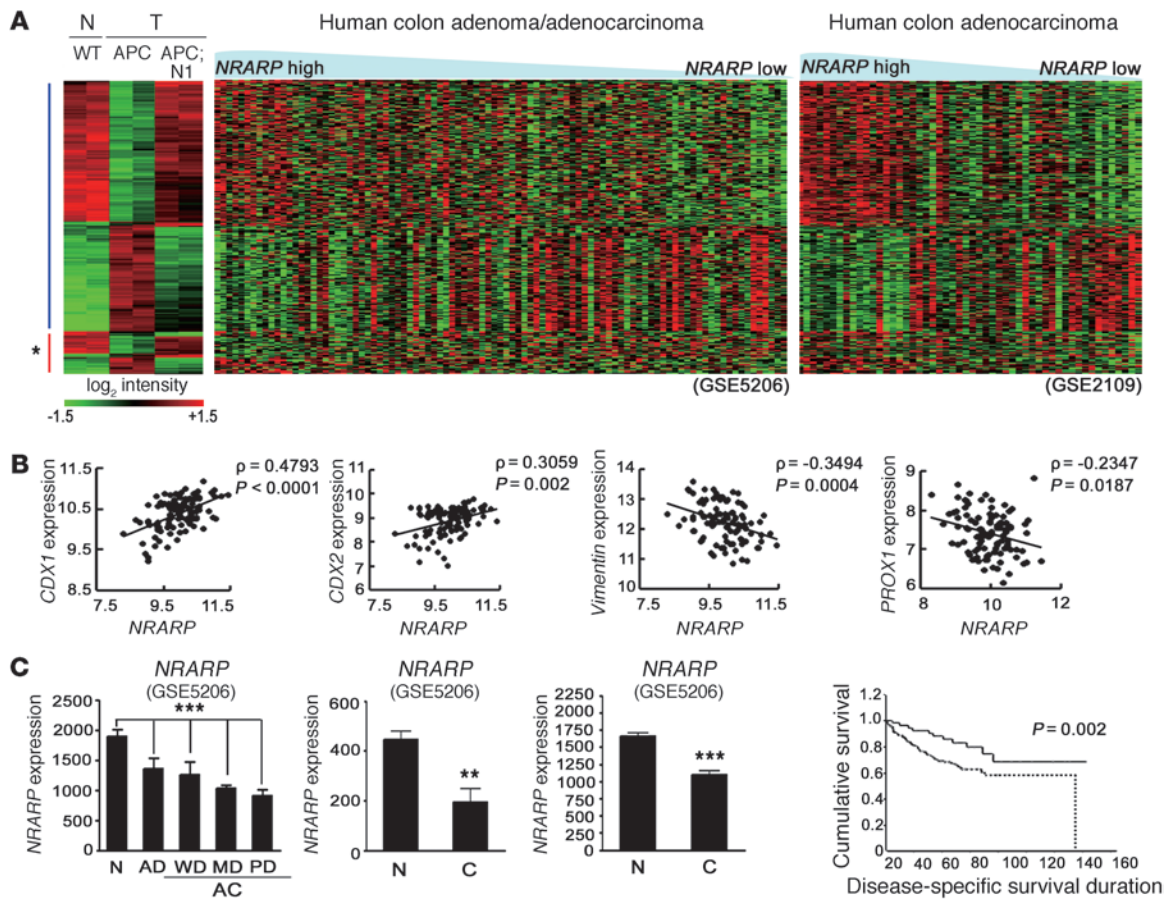
Figure 4
Conserved Notch signatures in both mouse and human intestinal tumors. (**A**) Heat map comparison between Notch-responsive genes (clusters A and B in Figure 3A) from mouse models and microarray data sets from human CRC patients (GEO GSE5206 and GSE2109). Note that genes upregulated upon Notch activation in Apc^{min} tumors have higher expression levels in $Nrarp^{hi}$ tumors compared with those of $Nrarp^{lo}$ tumors and vice versa. Asterisk indicates the group of genes that do not correlate between mouse and human data. APC, Vil-$Cre;Apc^{min}$. (**B**) Positive correlation of $CDX1$ and $CDX2$ (transcription factor for epithelial differentiation) and negative correlation of $VIMENTIN$ (epithelial-mesenchymal transition marker) and $PROX1$ (tumor progression related gene) with $Nrarp$, respectively. ρ, correlation coefficient. Statistics are by Pearson's correlation. (**C**) Expression levels of $Nrarp$ in the 3 independent microarray data sets (GEO GSE5206, GSE4107, and GSE 8671). AD, adenoma; AC, adenocarcinoma; WD, well differentiated; MD, moderately differentiated; PD, poorly differentiated; C, cancer. Note the reduced $Nrarp$ expression in CRCs compared with normal tissue. ***$P < 0.001$; **$P < 0.005$. Statistics for far-left graph are by ANOVA. (**D**) Positive correlation between $Nrarp$ expression and patient survival from microarray data set (GEO GSE17538). The Kaplan-Meier method was used to estimate survival of the 2 groups; $Nrarp^{hi}$ (solid line) and $Nrarp^{mid/lo}$ (dotted line).

or presence of cycloheximide (Figure 5C), indicating that the induction of NRARP by Notch activation in the $Nrarp^{hi}$ CRCLs does not require de novo protein synthesis. In accordance with the previous reports (22–24), our data show that $NRARP$ is a direct target of Notch signaling in the $Nrarp^{hi}$ CRCLs.

To determine whether the characteristics of CRCLs could be affected by Notch activity, $Nrarp^{hi}$ CRCLs were treated with DAPT. Surprisingly, $CDX1$ and $CDX2$ expression levels in $Nrarp^{hi}$ CRCLs, such as LOVO and SNU61, decreased following treatment with DAPT, whereas $VIMENTIN$ expression increased (Figure 5D). In contrast, when the $Nrarp^{lo/-}$ CRCLs SW620 and COLO205 were transfected with constitutively active Notch1 (ΔEN1), expression levels of $CDX1$ and $CDX2$ increased, while $VIMENTIN$ expression decreased (Figure 5D). Taken together, these results suggest that Notch activity affects the characteristics of CRCLs.

Since Notch signaling downregulates the WNT target genes $Axin2$, $Wif1$, $Nkd1$, and $Apcdd1$ in our mouse models (Figure 2, B–G), we further investigated whether Notch signaling also affects the expression of WNT target genes in human CRCLs. We determined whether inhibition of Notch signaling results in the expression of WNT target genes in $Nrarp^{hi}$ CRCLs. Interestingly, $PROX1$ expression was significantly increased by DAPT treatment in the $Nrarp^{hi}$ CRCLs SNU1040, SNU61, SNU283, LOVO, and SW480 (Figure 6A). Similar results were also obtained when dominant-negative mastermind-like (DN-MAML) gene, which blocks the transcriptional activity of Notch, was transfected into these CRCLs (Figure 6A). In addition to $PROX1$, other β-catenin–responsive genes, such as c-MYC and $Axin2$, were increased following DAPT treatment in LOVO and SNU61 cells, while expression of an unrelated gene, MMP-2, did not change (Figure 6B).
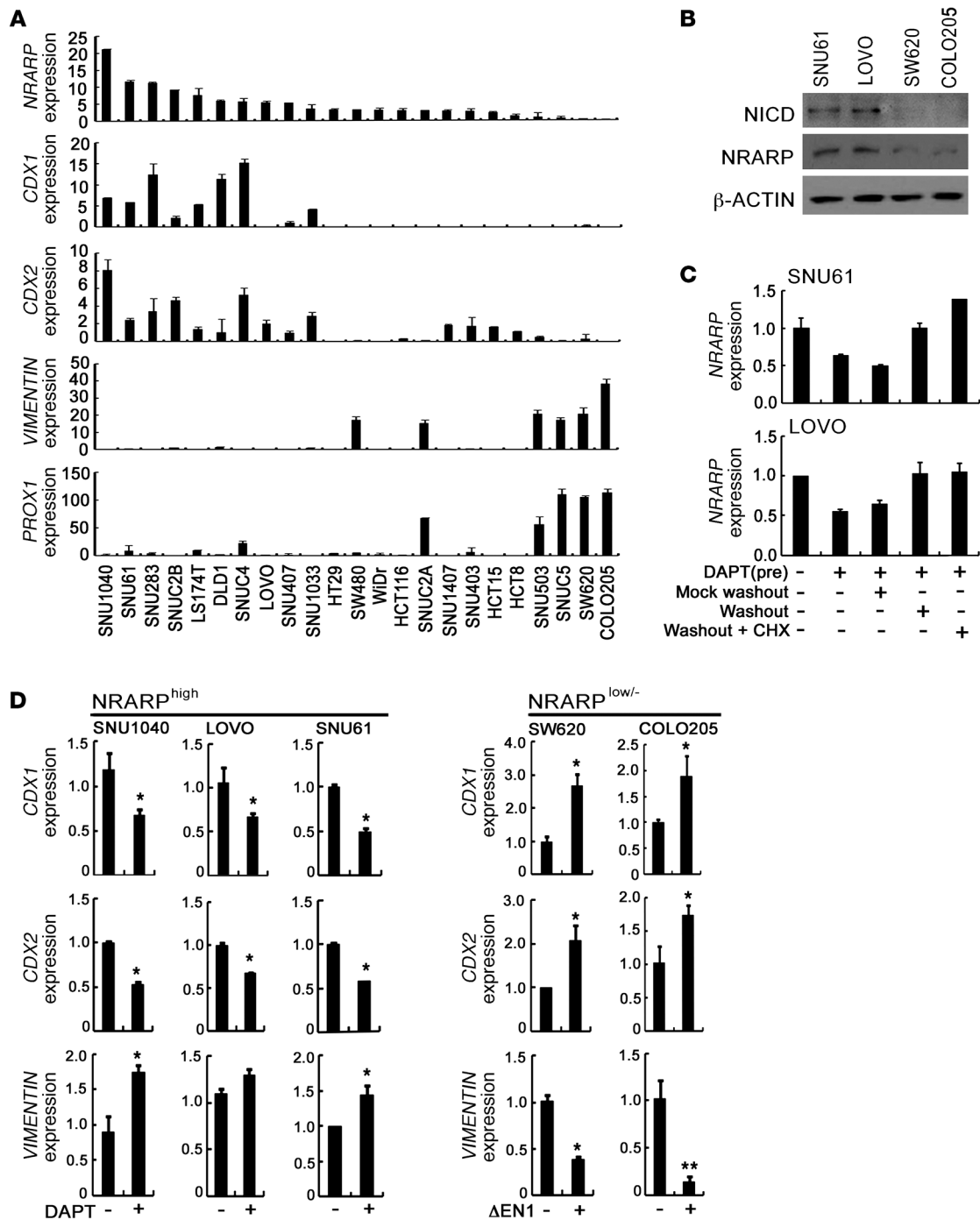
Figure 5
Notch signaling promotes differentiation of CRCLs. (**A**) Real-time qRT-PCR analysis of *Nrarp*, *CDX1*, *CDX2*, *VIMENTIN*, and *PROX1* in various human CRCLs. Note that *Nrarp*[hi] CRCLs showed high expression levels of *CDX1* and *CDX2*, while *Nrarp*^{lo/–} CRCLs highly expressed *VIMENTIN* and *PROX1*. (**B**) Western blot analysis of NICD and NRARP in CRCLs. Note that the expression of cleaved Notch 1 was well correlated with the expression levels of NRARP in SNU61, LOVO, SW620, and COLO205 cells. (**C**) Real-time qRT-PCR analysis of *Nrarp* expression in cycloheximide-treated CRCLs. LOVO and SNU61 cells were treated with DAPT (1 μM) for 48 hours to block Notch-signaling activity. Cells were then washed, and medium containing DAPT (mock washout) or medium lacking DAPT (washout) with or without 20 μM cycloheximide was added. After 12 hours of additional culture, cells were harvested, and *Nrarp* RNA levels were determined. (**D**) Real-time qRT-PCR analysis of CDX1, CDX2, and VIMENTIN in CRCLs. SNU1040, LOVO and SNU61 cells were treated daily with vehicle or 1 μM DAPT. SW620 and COLO205 cells were transfected with 2 μg of mock vector or ΔEN1, a constitutively active form of Notch1. Levels of CDX1, CDX2, and VIMENTIN transcripts were measured after 48 hours. Bars indicate mean + SD. *$P < 0.05$; **$P < 0.001$.
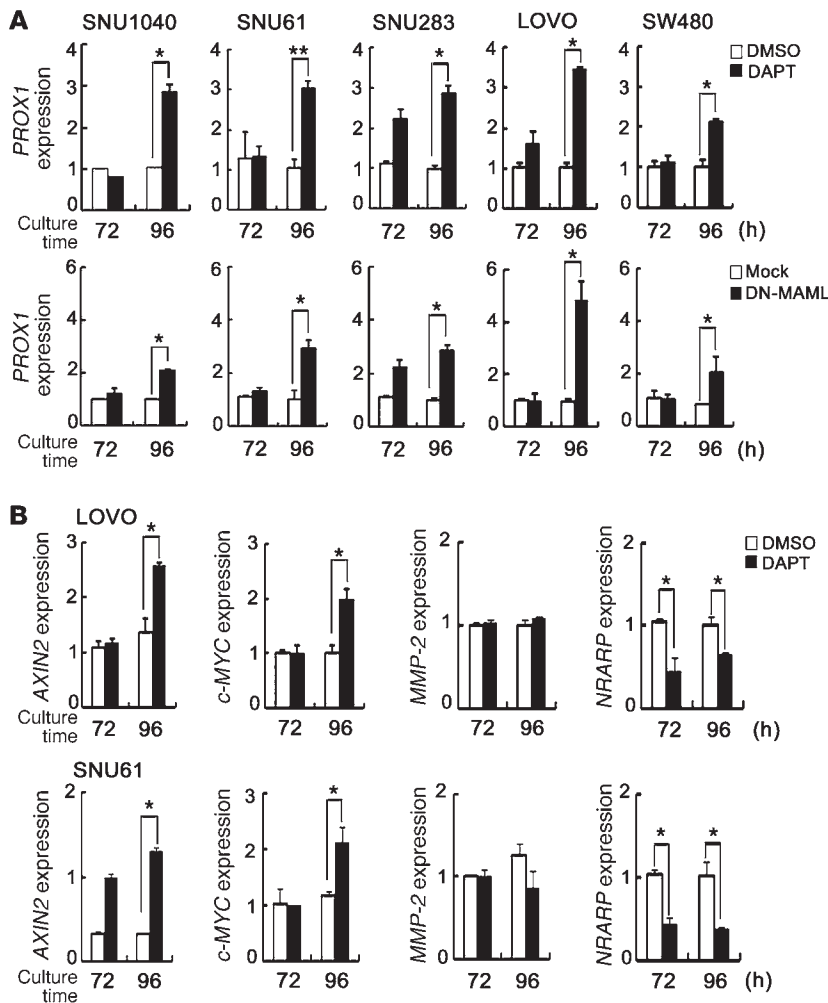
A

Figure 6
Inhibition of Notch signaling increases expression of WNT target genes in CRCLs. (**A**) Real-time qRT-PCR analysis of WNT target genes *PROX1* in *Nrarp^hi^* CRCLs. SNU1040, SNU61, SNU283, LOVO, and SW480 cells were treated daily with vehicle or 1 μM DAPT (upper graphs). Each cell was transfected with 2 μg of mock vector or DN-MAML (dominant-negative form of MAML) (lower graphs). Levels of *PROX1* transcripts were measured at the indicated times (72 and 96 hours). Bars indicate mean + SD. (**B**) Real-time qRT-PCR analysis of WNT target genes in DAPT-treated CRCLs. LOVO (upper graphs) and SNU61 (lower graphs) cells were treated daily with vehicle or 1 μM DATP. Levels of *Axin2* and *c-MYC* transcripts were measured at the indicated times (72 and 96 hours). *MMP2* and *Nrarp* were used for the control and Notch target genes, respectively. β-Actin was used for normalization. Bars indicate mean + SD. *$P < 0.05$; **$P < 0.001$.

B

We also determined whether activation of Notch signaling in *Nrarp^lo/−^* CRCLs leads to inhibition of WNT target gene expression. Expression levels of WNT/β-catenin target genes, including *PROX1*, *AXIN2*, *c-MYC*, and *APCDD1*, were decreased by ΔEN1 in SW620 and COLO205 CRCLs (Figure 7, A and B), while *MMP-2* expression did not change, suggesting that Notch signaling suppresses WNT target genes.

We next investigated whether Notch signaling influences tumor growth. As expected, the treatment of DAPT in the *Nrarp^hi^* SNU61 and LOVO CLCLs increased the proliferation of these cells, although the increase was not dramatic (Supplemental Figure 2A). Consistently, when ΔEN1 was expressed on the *NRARP^lo/−^* COLO205 and SW620 CRCLs, it significantly inhibited the proliferation of these CLCs (Supplemental Figure 2B). Taking these data together, we concluded that Notch signaling suppresses the expression of WNT target genes in human CRC cells.

Notch signaling suppresses the expression of WNT target genes by modifying epigenetic status. Since Notch signaling suppresses WNT/β-catenin activity under destruction complex–deregulated conditions, we speculated that Notch signaling could modulate the transcriptional activity of WNT target genes. To examine this possibility, we tested the binding activity of β-catenin/TCF4 to WNT/β-catenin target promoter regions. Interestingly, both DAPT treatment and DN-MAML overexpression in LOVO cells resulted in

increased binding activity of β-catenin/TCF4 to the *PROX1*, *Axin2*, and *c-MYC* promoter regions (Figure 8A and Supplemental Figure 3), suggesting that Notch activation affects the binding affinity of β-catenin/TCF4 to target gene promoters.

We next determined whether the binding affinity of β-catenin/TCF4 to the promoter is affected by Notch signaling through epigenetic modification. Deacetylation and methylation of histones play an important role in transcription regulation. Specifically, trimethylation of the histone H3 tail at lysine-9 (H3K9me3) and lysine-27 (H3K27me3) is associated with gene silencing, while trimethylation of the histone H3 tail at lysine-4 (H3K4me3) is associated with gene activation (29–31). The levels of H3K9me3 and H3K27me3 apparently decreased following DAPT treatment and overexpression of DN-MAML in LOVO cells, while H3K4me3, a marker of active gene transcription, increased (Figure 8A and Supplemental Figure 3). In contrast, the levels of H3K9me3 and H3K27me3 in *Nrarp^lo/−^* SW620 CRCLs apparently increased by ΔEN1 in WNT/β-catenin target promoter regions (Figure 8B and Supplemental Figure 4), while H3K4me3 and H3K4ac, markers of active genes, did not change (data not shown). These results show that Notch signaling can inhibit the expression of WNT/β-catenin target genes through epigenetic modification in CRC.

We further investigated how Notch signaling negatively regulates WNT target gene expression through histone modification.
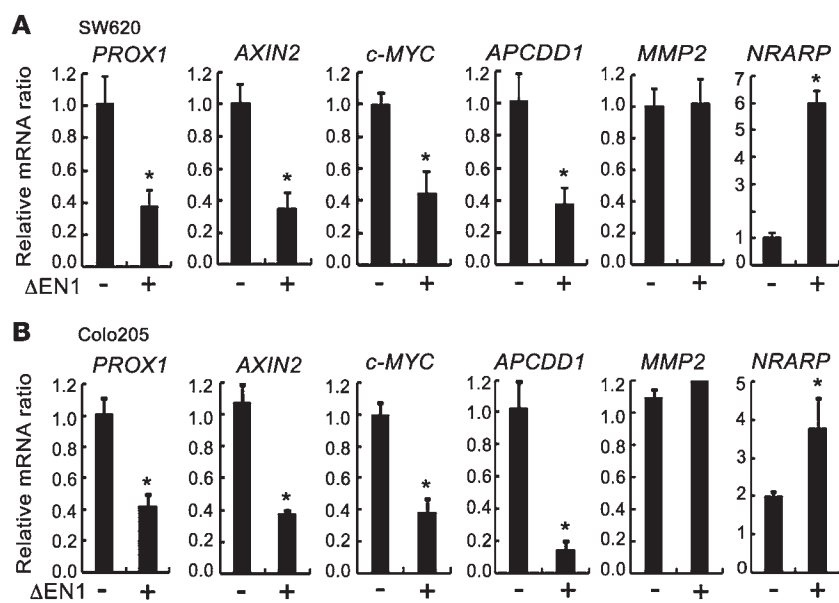
A SW620

B Colo205

Figure 7

Activation of Notch signaling downregulated expression of WNT target genes in CRCLs. (**A** and **B**) Real-time qRT-PCR analysis of WNT target genes (*PROX1*, *Axin2*, *c-MYC*, and *ApcDd1*) in *Nrarp*^{lo/−} CRCLs. SW620 and COLO205 cells were transfected with 2 μg of mock vector or ΔEN1. Levels of *PROX1*, *Axin2*, *c-MYC*, and *ApcDd1* transcripts were measured after 48 hours. *MMP2* and *Nrarp* were used as control and Notch target genes, respectively. β-Actin was used for normalization. Bars indicate mean + SD. *$P < 0.05$.

NLK, known to antagonize WNT signaling, acts downstream of the Notch pathway to inhibit TCF/β-catenin signaling during mesoderm induction in sea urchin embryos (32). NLK also phosphorylates SETDB1, a histone methyltransferase, leading to the formation of a corepressor complex that inactivates the activity of the transcriptional factor PPARγ through histone 3-K9 methylation (33). This suggests that NLK and SETDB1 affect Notch-mediated inhibition of WNT target gene expression by modifying histone status. To examine this possibility, we transfected *Nrarp*^{lo/−} SW620 cells with *NLK* siRNA and *SETDB1* siRNA (Supplemental Figure 5). These cells were then retransfected with control and ΔEN1. Intriguingly, downregulation of the WNT target genes *PROX1*, *c-MYC*, and *Axin2* by Notch signaling was significantly abolished by both *NLK* siRNA (Figure 8C) and *SETDB1* siRNA (Figure 8D) treatment, suggesting that NLK and SETDB1 are required for downregulation of WNT target genes by Notch signaling.

To investigate whether Notch signaling affects the recruitment of NLK and SETDB1 in WNT/β-catenin target promoter regions, we performed a ChIP assay using *Nrarp*^{lo/−} SW620 cells transfected with ΔEN1. As shown in Figure 8E, NLK and SETDB1 were readily recruited to WNT/β-catenin target promoter regions by ΔEN1. These results demonstrate that NLK and SETDB1 are involved in the epigenetic regulation of gene expression by Notch signaling.

Finally, we investigated the effects of DAPT in *NRARP*^{lo/−} CRCLs. As expected, we could not detect any significant differences in *NRARP*^{lo/−} CRCLs after DAPT treatment. Thus, we concluded that the DAPT treatment in the *NRARP*^{lo/−} cell lines did not further affect the epigenetic status and characteristics of these cells. A detailed Description is provided in Supplemental Information and Supplemental Figure 6.

Discussion

In the intestine, Notch signaling is a crucial signaling component for the maintenance of intestinal progenitors and stem cells and for the regulation of binary cell fate decisions (7, 8). Notch activation also significantly accelerates tumor formation in terms of number and onset timing (11). Since this signaling pathway has been shown to positively regulate the proliferation

of intestinal progenitors and the initiation of tumor formation, this pathway is defined as oncogenic. Generally, understanding the oncogenic role of specific signaling components is important for identifying therapeutic targets of cancers. Consequently, γ-secretase inhibitors, which were originally developed to treat Alzheimer patients, are also therapeutic candidates for the treatment of CRCs. However, our study shows that the role of Notch signaling in CRCs is complex. An incomplete understanding of the role of this pathway in CRC will prevent the successful development of treatment methods. Here, we discuss a new role for Notch in CRCs and the significance of this finding.

Dual roles of Notch signaling in intestinal tumorigenesis. Notch signaling is generally known to be oncogenic in various tissues, although the loss of this signaling can also result in tumor formation (34, 35). In the intestine, Notch signaling was thought to exhibit oncogenic potential by regulating the proliferation of intestinal progenitors (9, 36). In accordance with these reports, activation of Notch signaling strongly prompts tumorigenic activity in *Apc*[min] backgrounds (11, 12). We also observed that *Vil-Cre;RosaN1*[+/RNI];*Apc*[min] mice developed numerous tumors in the small and large intestines at an early age, and the onset of tumor formation was accelerated compared with that of control *Apc*[min] mice. Our results are consistent with a recent report stating that Notch and WNT signals cooperate to trigger intestinal tumorigenesis (11). Since a loss of heterozygosity (LOH) of the *Apc* locus is dependent upon centromeric somatic recombination (37, 38), a higher level of proliferation will increase the probability of acquiring this somatic mutation. Therefore, the increased tumor formation in Notch-activated epithelium may be caused by increased proliferation of intestinal progenitors (9).

Recently, Sonoshita et al. reported that disruption of Aes, a negative regulator of Notch signaling, in *Apc*[min] mice resulted in marked tumor invasion and intravasation, suggesting that Notch signaling may be critical for tumor metastasis when tumor cells interact with their surrounding endothelial cells and smooth muscle cells (39). However, tumor initiation and the number of tumor cells were not enhanced by genetic depletion of Aes in *Apc*[min] mice compared with control mice. Additionally, overexpression or knockdown of Aes did not affect the proliferation of colon cancer cells
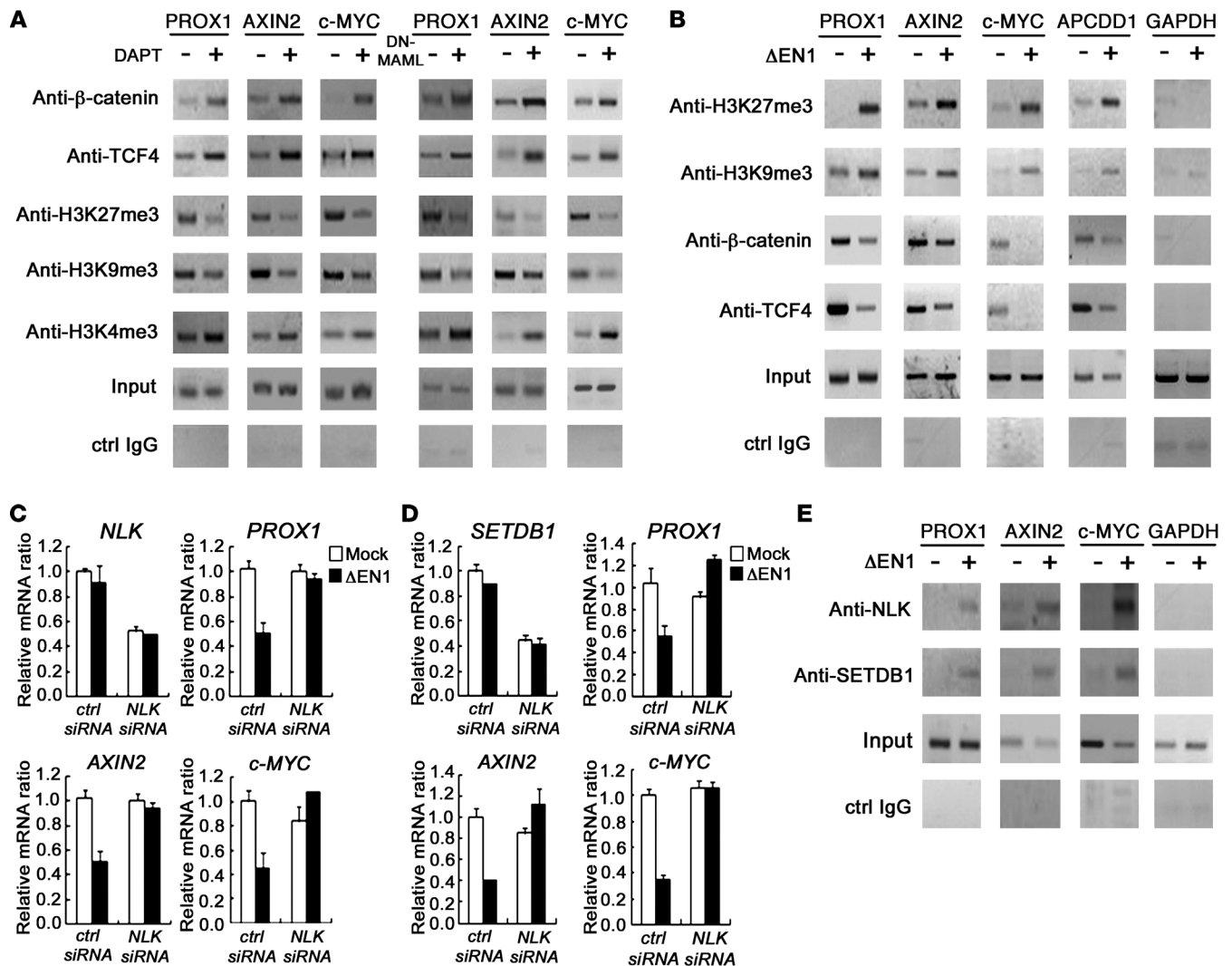
Figure 8
Notch signaling regulated expression of WNT target genes through epigenetic modification in CRCLs. (**A** and **B**) ChIP and PCR analysis of promoter regions of WNT target genes in *Nrarp^hi* LOVO cells and *Nrarp^lo/–* SW620 cells, and LOVO cells transfected with 2 μg of mock and DN-MAML (right panels) were treated for 96 hours. SW620 cells were transfected with 2 μg of mock vector or ΔEN1 for 48 hours. Soluble chromatin prepared from each cultured cells was immunoprecipitated with indicated Abs. The final DNA extracts were amplified using pairs of primers that cover the WNT/β-catenin–binding sites in promoter regions of WNT target genes. The exon 6 of *GAPDH* served as negative controls. (**C** and **D**) Real-time qRT-PCR analysis of WNT target genes (*PROX1*, *c-MYC*, and *Axin2*) in *Nrarp^lo/–* SW620 cells transfected with control siRNA, *NLK* siRNA, *SETDB1* siRNA, mock vector (white bars), and ΔEN1 (black bars), as indicated. Levels of *NLK*, *SETDB1*, *PROX1*, *Axin2*, and *c-MYC* transcripts were measured after 48 hours. (**E**) ChIP analysis of WNT target genes (*PROX1*, *c-MYC*, and *Axin2*) in *Nrarp^lo/–* SW620 cells. SW620 cells were transfected with 2 μg of mock vector or ΔEN1 for 48 hours. Soluble chromatin prepared from each cultured cells was immunoprecipitated with indicated Abs. The final DNA extracts were amplified using pairs of primers that cover the WNT/β-catenin binding sites in promoter regions of WNT target genes. The exon 6 of *GAPDH* served as a negative control.

in culture or in grafting experiments. These results are inconsistent with those of previous studies, demonstrating that activated Notch signaling facilitates tumor formation in *Apc^min* mice through increased proliferation of tumor cells (10, 11). Other studies have also reported that Aes can modulate other signaling pathways, such as WNT, TGF-β, and Hedgehog, which have critical roles in CRCs (40–42). Therefore, further characterization to determine whether Aes affects CRCs through Notch or other signaling pathways is required. Previously, Babaei-Jadidi et al. reported that the loss of *Fbxw7* in *Apc^min* mice resulted in early tumor initiation compared

with *Apc^min* mice (43). However, genetic deletion of *Fbxw7* in the intestine resulted in multiple deregulations of other molecules, such as Jun and DEK, as well as in Notch signaling. *Fbxw7* mutant tumors showed accumulation of the *DEK* protooncogene. Thus, it is not clear whether accelerated tumor initiation in *Fbxw7* in *Apc^min* mice is due to activated Notch1.

In the present study, we directly activated Notch signaling in *Apc^min* mice using the *RosaN1^+/RN1* knockin mouse, with which we could activate components downstream of Notch and rescue and/or reverse the loss-of-Notch mutant phenotype (44). Histological

analysis of *Vil-Cre;RosaN1⁺/RN1;Apcᵐⁱⁿ* mice revealed that Notch-activated tumors in these mice exhibit low-grade adenoma characteristics despite an initial increase in tumor formation. Additionally, Notch activation can revert approximately 40% of gene expression changes associated with *Apcᵐⁱⁿ* tumors. The most striking finding was that WNT/β-catenin target gene expression was downregulated upon activation of Notch in *Apcᵐⁱⁿ* tumors. This was also demonstrated in human CRCs and CRCLs. Furthermore, we found that Notch signaling regulates the expression of WNT/β-catenin target genes through epigenetic modification in CRC cells. Based on this observation, our present study demonstrates that Notch signaling acts negatively on CRC progression through downregulation of WNT/β-catenin target genes, which explains how Notch-activated *Apcᵐⁱⁿ* tumor remains in a low-grade state.

Crosstalk between Notch and WNT signaling in intestinal tumorigenesis and Nrarp, a reliable marker for Notch signaling activity. Several genetic observations suggest that functional crosstalk exists between WNT and Notch signaling (45). Initial insights on how Notch signaling represses WNT signaling arose from studies conducted using *Drosophila*, in which a direct physical interaction between NICD and Dishevelled has been suggested as mediating the mutual inhibition of these 2 signaling pathways (46). In the skin, Notch1 activation inhibits the WNT signaling pathway by downregulating WNT ligand gene expression, which is mediated by p21 transcription (47). Additionally, GSK3β has been suggested to be a crucial link between these 2 signaling pathways (44, 48, 49). However, downregulation of WNT/β-catenin target genes in *Apcᵐⁱⁿ* tumors by active Notch signaling is not easily explained by such mechanisms because they are upstream regulators of the APC/β-catenin complex. Here, we observed molecular crosstalk between WNT and Notch signaling, which takes place downstream of the APC/β-catenin complex; Notch signaling can suppress the transcriptional activity of WNT target genes by modulating their histone status. Additionally, the negative correlation between Notch and WNT activity was observed in our animal model as well as in human CRC patient arrays and human CRCLs.

Recently, Alves-Guerra et al. reported that MAML1 is a coactivator of β-catenin activity and that the C-terminal region of MAML1 (aa 640–840) is critical to β-catenin activity (50). In our study, we used DN-MAML (aa 13–74) to block Notch activity by binding to NICD. When DN-MAML (aa 13–74) was transiently expressed in various *NRARPʰⁱ* colon cancer cells, it did not affect β-catenin activity, while Notch activity was effectively blocked. Our data show that the N-terminal domain of MAML1 is not required for β-catenin activity. Alves-Guerra et al. also demonstrated that the increase in transcriptional activity of the β-catenin pathway is due to MAML in addition to crosstalk with the Notch signaling pathway. However, we observed that γ-secretase inhibitor (DAPT) treatment of *NRARPʰⁱ* colon cancer cells inhibited Notch activity similarly to DN-MAML (aa 13–74), suggesting that the expression of WNT/β-catenin target genes is regulated in a Notch signaling–dependent manner in *Nrarpʰⁱ* CRCLs.

The best characterized targets of Notch-mediated activation include members of the hairy and enhancer of split (HES) and HES-related repressor protein (HERP) families of basic helix-loop-helix (bHLH) transcriptional repressors (51). Although *Hes1* is a well-known Notch target gene, it is also regulated by Notch-independent signaling pathways, such as the WNT pathway. Recently, Peignon et al. reported that *Hes1* was induced directly by β-catenin signaling via the conserved Tcf-binding site of the *Hes1* promoter

region (14). Indeed, *Hes1* expression is elevated in *Apcᵐⁱⁿ* tumors and human CRCs (10). Moreover, *Hes1* expression is not decreased in *Apc* and *Rbp* double-knockout mice compared with *Apc*-null mice (14). In this study, we identified *Nrarp* as a reliable Notch target gene for representing the endogenous level of Notch signaling activity in intestinal tumors. *Nrarp* is a Notch target gene for feedback inhibition of its transcriptional activity. Notch signaling activity influences the expression of *Nrarp* as it does other feedback inhibitors such as *Axin2* (WNT/β-catenin signaling) and *Socs3* (Jak/Stat3 signaling) (17). The expression level of Nrarp is significantly reduced in *Notch1⁻/⁻* embryos (24). Moreover, the expression of *Nrarp*, but not *Hes1*, was well correlated with the expressional changes of a TNR (*TNR-GFP*) (Figure 3A). These data show that *Nrarp* is a reliable sensitivity and dependency marker for Notch signaling activity.

In conclusion, we demonstrate the dual roles of Notch signaling in intestinal tumor progression; Notch both suppresses tumor progression and enhances tumor initiation. In particular, Notch signaling has a negative effect on CRC progression by downregulating WNT/β-catenin target genes. Thus, the results of our study will help further the understanding of the dual roles of Notch signaling in intestinal tumorigenesis and provide critical clues for improving treatments for colonic neoplasia and cancers. We are only beginning to understand the complex interplay between these signaling pathways, and further studies will reveal more detailed mechanisms by which crosstalk contributes to intestinal tumor progression. This will help us to unveil a promising tool for restoring the deregulated WNT pathway in CRCs.

Methods

Mice. The *Apcᵐⁱⁿ* mouse line and *Villin-Cre* (*Vil-Cre*) transgenic mouse line were purchased from The Jackson Laboratories and maintained in our animal colony under our institutional guidelines. *Rosa-Notch1* mice (a gift from D. Melton, Harvard Stem Cell Institute, Harvard University, Boston, Massachusetts, USA) harbor the intracellular domain of mouse Notch1 in the ubiquitously expressed *Rosa26* locus, the expression of which is blocked in the absence of Cre. *Rosa-Notch1* mice were crossed with the *Vil-Cre* mice and *Apcᵐⁱⁿ* mice to generate *Vil-Cre;RosaN1⁺/RN1;Apcᵐⁱⁿ*. The *TNR* mice were a gift from N. Gaiano (Johns Hopkins University, Institute for Cell Engineering, School of Medicine, Baltimore, Maryland, USA).

Cell culture. Human CRC cells were obtained from ATCC and the Korean Cell Line Bank (52). Cells were maintained in RPMI 1640 medium (100 U/ml penicillin; 100 μg/ml streptomycin) supplemented with 10% FBS (HyClone Labs) in an atmosphere of 95% air and 5% CO_2 at 37°C. All experiments were performed with cells at 50%–70% confluence.

Tissue preparation, immunohistochemistry, and in situ hybridization. The intestinal tract was flushed gently with cold PBS, followed by a flush with 4% paraformaldehyde in PBS. For histological analysis, tissues were fixed in 4% paraformaldehyde overnight at 4°C and embedded in paraffin wax for sectioning. Sections (3–4 μm) were stained using H&E. For immunohistochemistry, paraffin-embedded sections were rehydrated, and antigenic epitopes were exposed using boiling citrate buffer or Tris/EDTA buffer. Sections were incubated in blocking solution (3% BSA, 5% goat serum or horse serum, and 0.5% Tween 20 in PBS) at room temperature (RT) for 2 hours, followed by an additional incubation with Abs to β-catenin (1:200, BD Biosciences; 1:200, Santa Cruz Biotechnology Inc.), E-cadherin (1:200, BD Biosciences), α-catenin (1:50, Santa Cruz Biotechnology Inc.), ZO-1 (1:200, Zymed), Prox1 (1:100, Millipore), Axin2 (1:200, Abcam), and Apcdd1 (1:200, Abcam). Specific binding was detected using an Envision kit (DAKO) or Alexa Fluor 488–labeled (green) and/or Alexa

Fluor 594–labeled (red) Abs (Molecular Probes). For in situ hybridization, tissues were fixed in 10% formalin overnight at RT and embedded in paraffin wax for sectioning. Dig-labeled antisense RNA transcripts were used for hybridization and visualized using anti-Dig-alkaline phosphatase Ab (BM) and BM purple reagent (BM).

Microarray analysis and statistics. For mouse tissue mRNA analysis, total RNA was isolated using TRIZOL (Invitrogen) and purified using RNeasy columns (QIAGEN). The RNA was reverse transcribed, amplified, and hybridized onto Sentrix Mouse-6 v1 BeadChips (Illumina) according to the manufacturer's instructions. Probe intensity was normalized using the quantile method (53) at the $\log_2$ scale. To identify tumor DEGs (T-DEG), fold changes between WT normal tissues and *Apc^min* tumors were computed, and *P* values were calculated against null fold changes generated by 100 permutations of sample labels. T-DEG was defined as a set of genes having fold changes greater than plus or minus 2 and *P* values of less than 0.05. Notch-DEG was identified using the same method. To identify genes whose expression levels correlated with that of *Nrarp* in 2 microarray data sets, we first calculated Pearson's and Spearman's correlations between *Nrarp* and other genes in each data set (GEO GSE2109 and GSE5206). We then calculated the *P* values for each type of correlation using null correlations between *Nrarp* and randomly permuted genes. Random permutation experiments were repeated 100 times. For each gene in the data set, 2 *P* values from Pearson's and Spearman's correlations were integrated into a combined *P* value by using the Liptak-Stouffer Z-method (54). Finally, 2 combined *P* values from 2 data sets were recombined to generate an overall *P* value, which indicates the significance of correlation of a gene with *Nrarp* in both data sets. Human *NRARP* CO-DEG was then identified as a gene with an overall *P* value of less than 0.05. KEGG pathways significantly associated with a set of genes were identified using the Database for Annotation, Visualization, and Integrated Discovery (DAVID) (55).

Retroviral expression vectors and siRNAs. The ΔEN1 cDNA was cloned into the *Hpa*I site of pMSCV. ΔEN1 is a constitutively active form of Notch1 that lacks the extracellular domain. This form of Notch1 can bypass S2 cleavage and is readily processed by γ-secretase in a ligand-independent manner, but can still be blocked by a γ-secretase inhibitor. The MigR1-DN-MAML (dominant-negative form of MAML1) was a gift of J. Aster (Brigham and Women's Hospital, Boston, Massachusetts, USA). siRNA to *NLK* and *SETDB1* was designed and synthesized by Dharmacon (Thermo Scientific).

Western blot and RT-PCR analyses. For Western blot analysis, equal amounts of whole-cell extracts or tissue extracts were separated using SDS-PAGE and transferred to PVDF membranes. Membranes were incubated with Abs to Mib1 (gift from P. Gallagher, Department of Cellular and Integrative Physiology, Indiana University School of Medicine, Indianapolis, Indiana, USA), cleaved Notch1 (Abcam), Hes1 (gift from T. Sudo, Pharmaceutical Research Laboratories, Toray Industries Inc., Tebiro, Kamakura, Japan), Math1 (Abcam), NRARP (BD Biosciences — Clontech), Prox1 (Chemicon), Axin2 (Abcam),

C-myc (Santa Cruz Biotechnology Inc.), APCDD1 (Abcam), MMP2 (Cell Signaling Technology), and β-actin (Sigma-Aldrich). Protein bands were detected by enhanced chemiluminescence (Amersham Biosciences). For RT-PCR and real-time qRT-PCR analysis, total RNA was isolated from freshly dissected intestines using TRIZOL reagent (Life Technologies), and complementary DNA synthesis was performed according to the manufacturer's instructions (Omniscript Kit; QIAGEN). PCR quantification was conducted using the SYBR green method. Primer information is available in Supplemental Data.

ChIP analysis. ChIP analyses were performed using the EZ-Chip kit according to the manufacturer's protocol (Upstate Biotechnology). Specific PCR primers were designed to contain putative β-catenin/TCF4–binding sites as determined by TFSEARCH, version. 1.3, and MatInspector, version 3.0, Genomatix Software. Immunoprecipitation was performed using Abs to β-catenin (Santa Cruz Biotechnology Inc.), TCF-4 (Santa Cruz Biotechnology Inc.), H3K27me3 (Abcam), H3K9me3 (Abcam), H3K4me3 (Abcam), NLK (Abcam), and SETDB1 (Abcam). Immunoprecipitated complexes were isolated and 1 μl of immunoprecipitated purified DNA was amplified using pairs of primers that cover the WNT/β-catenin–binding sites in promoter regions of WNT target genes. Exon 6 of GAPDH served as a negative control. Primer information is available in the Supplemental Data.

Statistics. All values are given as mean ± SD. Statistical comparisons were made by 2-tailed Student's *t* test. A *P* value of less than 0.05 was considered to be statistically significant.

Study approval. All mouse lines were maintained in specific pathogen–free conditions at the Institute of Laboratory Animal Resources, Seoul National University. All animal experiments were approved by the ethical committees at Seoul National University (permit number SNU-081001-9).

Address correspondence to: Young-Yun Kong, Department of Biological Sciences, Seoul National University, 599 Gwanak-ro, Gwanak-gu, Seoul, 151-747, Republic of Korea. Phone: 82.2.880.2638; Fax: 82.2.872.1993; E-mail: ykong@snu.ac.kr.

1. Fodde R, Smits R, Clevers H. APC, signal transduction and genetic instability in colorectal cancer. *Nat Rev Cancer*. 2001;1(1):55–67.

2. Kinzler KW, Vogelstein B. Lessons from hereditary colorectal cancer. *Cell*. 1996;87(2):159–170.

3. Grady WM, Carethers JM. Genomic and epigenetic instability in colorectal cancer pathogenesis. *Gastroenterology*. 2008;135(4):1079–1099.

4. Sancho E, Batlle E, Clevers H. Signaling pathways in intestinal development and cancer. *Annu Rev Cell Dev Biol*. 2004;20:695–723.

5. Katoh M. Networking of WNT, FGF, Notch, BMP, and Hedgehog signaling pathways during carcinogenesis. *Stem Cell Rev*. 2007;3(1):30–38.

6. van de Wetering M, et al. The beta-catenin/TCF-4 complex imposes a crypt progenitor phenotype on colorectal cancer cells. *Cell*. 2002;111(2):241–250.

7. Nakamura T, Tsuchiya K, Watanabe M. Crosstalk between Wnt and Notch signaling in intestinal epithelial cell fate decision. *J Gastroenterol*. 2007;42(9):705–710.

8. Vooijs M, Liu Z, Kopan R. Notch: architect, landscaper, and guardian of the intestine. *Gastroenterology*. 2011;141(2):448–459.

9. Fre S, Huyghe M, Mourikis P, Robine S, Louvard D, Artavanis-Tsakonas S. Notch signals control the fate of immature progenitor cells in the intestine. *Nature*. 2005;435(7044):964–968.

10. van Es JH, et al. Notch/gamma-secretase inhibition turns proliferative cells in intestinal crypts and adenomas into goblet cells. *Nature*. 2005;435(7044):959–963.

11. Fre S, et al. Notch and Wnt signals cooperatively control cell proliferation and tumorigenesis in the intestine. *Proc Natl Acad Sci U S A*. 2009; 106(15):6309–6314.

12. Rodilla V, et al. Jagged1 is the pathological link between Wnt and Notch pathways in colorectal cancer. *Proc Natl Acad Sci U S A*. 2009;106(15):6315–6320.

13. Akiyoshi T, et al. Gamma-secretase inhibitors enhance taxane-induced mitotic arrest and apoptosis in colon cancer cells. *Gastroenterology*. 2008; 134(1):131–144.

14. Peignon G, et al. Complex interplay between beta-catenin signalling and Notch effectors in intestinal tumorigenesis. *Gut*. 2011;60(2):166–176.

15. Murtaugh LC, Stanger BZ, Kwan KM, Melton DA. Notch signaling controls multiple steps of pancreatic differentiation. *Proc Natl Acad Sci U S A*. 2003; 100(25):14920–14925.

16. Madison BB, Dunbar L, Qiao XT, Braunstein K,

Braunstein E, Gumucio DL. Cis elements of the villin gene control expression in restricted domains of the vertical (crypt) and horizontal (duodenum, cecum) axes of the intestine. *J Biol Chem*. 2002;277(36):33275–33283.

17. Jho EH, Zhang T, Domon C, Joo CK, Freund JN, Costantini F. Wnt/beta-catenin/Tcf signaling induces the transcription of Axin2, a negative regulator of the signaling pathway. *Mol Cell Biol*. 2002; 22(4):1172–1183.

18. Takahashi M, et al. Isolation of a novel human gene, APCDD1, as a direct target of the beta-Catenin/T-cell factor 4 complex with probable involvement in colorectal carcinogenesis. *Cancer Res*. 2002;62(20):5651–5656.

19. Yan D, et al. Elevated expression of axin2 and hnkd mRNA provides evidence that Wnt/beta -catenin signaling is activated in human colon tumors. *Proc Natl Acad Sci U S A*. 2001;98(26):14973–14978.

20. Zirn B, et al. Target genes of the WNT/beta-catenin pathway in Wilms tumors. *Genes Chromosomes Cancer*. 2006;45(6):565–574.

21. Petrova TV, et al. Transcription factor PROX1 induces colon cancer progression by promoting the transition from benign to highly dysplastic phenotype. *Cancer Cell*. 2008;13(5):407–419.

22. Pirot P, van Grunsven LA, Marine JC, Huylebroeck D, Bellefroid EJ. Direct regulation of the Nrarp gene promoter by the Notch signaling pathway. *Biochem Biophys Res Commun*. 2004;322(2):526–534.

23. Lamar E, et al. Nrarp is a novel intracellular component of the Notch signaling pathway. *Genes Dev*. 2001;15(15):1885–1899.

24. Krebs LT, Deftos ML, Bevan MJ, Gridley T. The Nrarp gene encodes an ankyrin-repeat protein that is transcriptionally regulated by the notch signaling pathway. *Dev Biol*. 2001;238(1):110–119.

25. Duncan AW, et al. Integration of Notch and Wnt signaling in hematopoietic stem cell maintenance. *Nat Immunol*. 2005;6(3):314–322.

26. Soubeyran P, et al. Cdx1 promotes differentiation in a rat intestinal epithelial cell line. *Gastroenterology*. 1999;117(6):1326–1338.

27. Chen X, Halberg RB, Burch RP, Dove WF. Intestinal adenomagenesis involves core molecular signatures of the epithelial-mesenchymal transition. *J Mol Histol*. 2008;39(3):283–294.

28. Smith JJ, et al. Experimentally derived metastasis gene expression profile predicts recurrence and death in patients with colon cancer. *Gastroenterology*. 2010;138(3):958–968.

29. Lachner M, O'Carroll D, Rea S, Mechtler K, Jenuwein T. Methylation of histone H3 lysine 9 creates a binding site for HP1 proteins. *Nature*. 2001;410(6824):116–120.

30. Nakayama J, Rice JC, Strahl BD, Allis CD, Grewal SI. Role of histone H3 lysine 9 methylation in epigenetic control of heterochromatin assembly. *Science*. 2001;292(5514):110–113.

31. Schotta G, et al. Central role of Drosophila SU(VAR)3-9 in histone H3-K9 methylation and heterochromatic gene silencing. *EMBO J*. 2002;21(5):1121–1131.

32. Rottinger E, Croce J, Lhomond G, Besnardeau L, Gache C, Lepage T. Nemo-like kinase (NLK) acts downstream of Notch/Delta signalling to downregulate TCF during mesoderm induction in the sea urchin embryo. *Development*. 2006; 133(21):4341–4353.

33. Takada I, et al. A histone lysine methyltransferase activated by non-canonical Wnt signalling suppresses PPAR-gamma transactivation. *Nat Cell Biol*. 2007;9(11):1273–1285.

34. Ranganathan P, Weaver KL, Capobianco AJ. Notch signalling in solid tumours: a little bit of everything but not all the time. *Nat Rev Cancer*. 2011;11(5):338–351.

35. Radtke F, Raj K. The role of Notch in tumorigenesis: oncogene or tumour suppressor? *Nat Rev Cancer*. 2003;3(10):756–767.

36. Riccio O, et al. Loss of intestinal crypt progenitor cells owing to inactivation of both Notch1 and Notch2 is accompanied by derepression of CDK inhibitors p27Kip1 and p57Kip2. *EMBO Rep*. 2008;9(4):377–383.

37. Luongo C, Moser AR, Gledhill S, Dove WF. Loss of Apc+ in intestinal adenomas from Min mice. *Cancer Res*. 1994;54(22):5947–5952.

38. Shoemaker AR, Luongo C, Moser AR, Marton LJ, Dove WF. Somatic mutational mechanisms involved in intestinal tumor formation in Min mice. *Cancer Res*. 1997;57(10):1999–2006.

39. Sonoshita M, et al. Suppression of colon cancer metastasis by Aes through inhibition of Notch signaling. *Cancer Cell*. 2011;19(1):125–137.

40. Chen G, Courey AJ. Groucho/TLE family proteins and transcriptional repression. *Gene*. 2000; 249(1–2):1–16.

41. Wang WF, Wang YG, Reginato AM, Plotkina S, Gridley T, Olsen BR. Growth defect in Grg5 null mice is associated with reduced Ihh signaling in growth plates. *Dev Dyn*. 2002;224(1):79–89.

42. Roose J, et al. The Xenopus Wnt effector XTcf-3 interacts with Groucho-related transcriptional repressors. *Nature*. 1998;395(6702):608–612.

43. Babaei-Jadidi R, et al. FBXW7 influences murine intestinal homeostasis and cancer, targeting Notch, Jun, and DEK for degradation. *J Exp Med*. 2011;208(2):295–312.

44. Koo BK, et al. Notch signaling promotes the generation of EphrinB1-positive intestinal epithelial cells. *Gastroenterology*. 2009;137(1):145–155.

45. Hayward P, Kalmar T, Arias AM. Wnt/Notch signalling and information processing during development. *Development*. 2008;135(3):411–424.

46. Axelrod JD, Matsuno K, Artavanis-Tsakonas S, Perrimon N. Interaction between Wingless and Notch signaling pathways mediated by dishevelled. *Science*. 1996;271(5257):1826–1832.

47. Devgan V, Mammucari C, Millar SE, Brisken C, Dotto GP. p21WAF1/Cip1 is a negative transcriptional regulator of Wnt4 expression downstream of Notch1 activation. *Genes Dev*. 2005; 19(12):1485–1495.

48. Foltz DR, Santiago MC, Berechid BE, Nye JS. Glycogen synthase kinase-3beta modulates notch signaling and stability. *Curr Biol*. 2002; 12(12):1006–1011.

49. Brack AS, Conboy IM, Conboy MJ, Shen J, Rando TA. A temporal switch from notch to Wnt signaling in muscle stem cells is necessary for normal adult myogenesis. *Cell Stem Cell*. 2008;2(1):50–59.

50. Alves-Guerra MC, Ronchini C, Capobianco AJ. Mastermind-like 1 Is a specific coactivator of beta-catenin transcription activation and is essential for colon carcinoma cell survival. *Cancer Res*. 2007;67(18):8690–8698.

51. Iso T, Kedes L, Hamamori Y. HES and HERP families: multiple effectors of the Notch signaling pathway. *J Cell Physiol*. 2003;194(3):237–255.

52. Ku JL, Park JG. Biology of SNU cell lines. *Cancer Res Treat*. 2005;37(1):1–19.

53. Bolstad BM, Irizarry RA, Astrand M, Speed TP. A comparison of normalization methods for high density oligonucleotide array data based on variance and bias. *Bioinformatics*. 2003;19(2):185–193.

54. Hwang D, et al. A data integration methodology for systems biology. *Proc Natl Acad Sci U S A*. 2005;102(48):17296–17301.

55. Huang da W, Sherman BT, Lempicki RA. Systematic and integrative analysis of large gene lists using DAVID bioinformatics resources. *Nat Protoc*. 2009;4(1):44–57.